ICANS-XV
15th Meeting of the International Collaboration on Advanced Neutron Sources
November 6-9, 2000
Tsukuba, Japan

10.1
First Results from the MAPS spectrometer at ISIS

C.D.Frost[1]* and T.G.Perring[1]

[1]ISIS Facility, CLRC Rutherford Appleton Laboratory, Didcot, Oxon OX11 0QX, UK
*E-mail: c.d.frost@rl.ac.uk

Abstract

The scientific commissioning of MAPS, the new state-of-the-art neutron scattering instrument at ISIS, has just begun. The design of MAPS has been optimised for studies of coherent excitations in single-crystals. The principal innovation is the use of position sensitive detectors that provide close to continuous coverage over a large solid angle detector array in the forward direction. The technical description of the spectrometer is presented, and examples from the first scientific experiments are used to illustrate how the position sensitive detectors coupled with easy-to-use visualisation software is already beginning to have an impact in the measurement of excitations in single crystals.

I. Introduction

MAPS, the new direct geometry time-of-flight chopper spectrometer at ISIS, has completed its technical commissioning and has entered a phase of scientific commissioning. MAPS builds on the heritage of HET and MARI [1,2], which have been at the forefront of explorations of excitations on high-flux pulsed spallation neutron sources. The fundamental difference between MAPS and its predecessors is that it has been optimised for experiments with single crystals.

Single crystals allow the generalised magnetic susceptibility, $\chi''(\mathbf{q},\omega)$, which contains the full information on the nature of the magnetic interactions within a material, to be measured without the loss of information that powder averaging forces. Over the past decade, an increasing amount of time on HET and MARI has been devoted to such single crystal measurements (a rise from 0% to 50% of beamtime in that decade), which take advantage of the low background and good energy resolution of these spectrometers, particularly at high incident neutron energies. Many successful studies have been made in 1D, 2D and 3D magnetic systems ranging from realisation of model magnetic systems, high temperature superconductors to transition metals magnets and colossal magnetoresistive manganites [3-9].

The HET and MARI spectrometers were not, however, principally designed for single crystal experiments. Two aspects of the detector array on these spectrometer have imposed limitations on their effectiveness at single crystal studies:

- The structural elements of the detector tank (the vacuum vessel that evacuates the sample to detector flight path) generate gaps in the detector coverage. The kinematic constraints frequently result in important parts of the spectrum being coincident with these gaps.

- The detectors used on HET and MARI are mostly 30cm long ^{3}He proportional gas detectors that integrate the signal along their length. Frequently this integration does not coincide to any particularly special direction in reciprocal space, and can be over a large volume of reciprocal space (especially at high energies), which overwhelms the intrinsic instrumental resolution in that direction.

The concept of a direct geometry spectrometer at ISIS for single crystal studies has one principle at the heart of the design – control of the resolution. On MAPS this is achieved by using a large position sensitive detector array with almost complete coverage over 16m^2. The collection, manipulation and visualisation of the data from this vast array has only been possible through the predicted rise in technology and computing power between conception and completion of the spectrometer.

The bold step of constructing MAPS was realised thorough a grant awarded by the UK Engineering and Physical Science Research Council. MAPS soon attracted international recognition with contributions from Japan and the USA. In Section II the design of MAPS is presented and in Section III data from the first experiments conducted on the spectrometer is described.

II. MAPS Design

A diagram of the MAPS spectrometer is shown in figure 1, and the principal parameters are given in table 1.

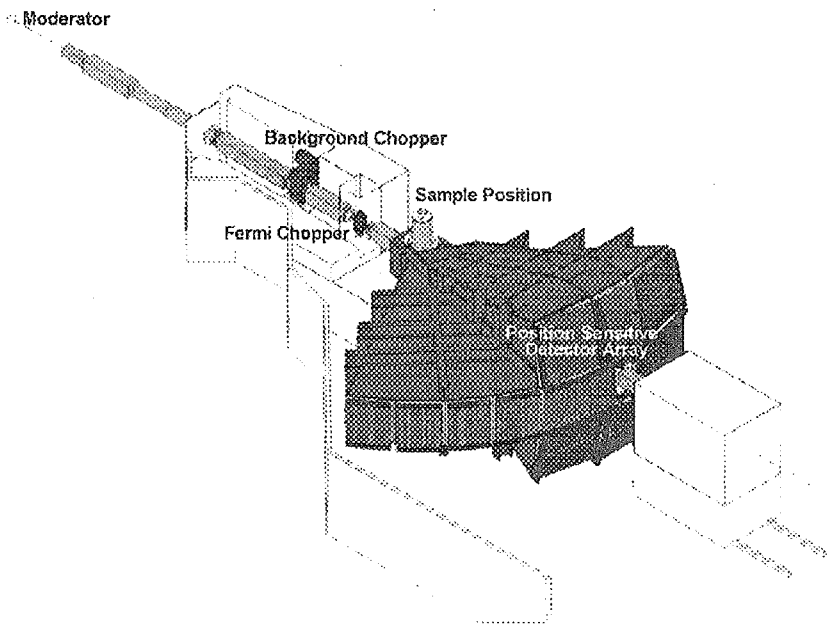

Figure 1: Diagram of the MAPS spectrometer

Table 1: MAPS Instrument Parameters

Beamline	S1
Moderator	300K water poisoned moderator
Incident energy	15-2000 meV
Energy resolution	Depends on the choice of Fermi chopper $\Delta \hbar\omega / E_i$ = 2 – 5% FWHM at elastic line ($\hbar\omega$ = 0) ≈ 1.5% FWHM at full energy transfer ($\hbar\omega = E_i$)
Moderator to sample distance	12.00m
Sample to detector distance	6.00m
Fermi Chopper	10.20 m from moderator 50-600 Hz phased to ISIS pulse ± 0.1μ s Several chopper packages are available optimised for different incident energy and resolution requirements
Background chopper	8.5m at 50 Hz or 100 Hz
Beam size at sample	55mm x 55mm, motorised jaws can define smaller beam sizes
Detectors	6 m from sample position 16m^2 array of 147,456 pixel elements Low angle bank 3-20º, 30º in the corners High angle bank 20-60º 1m tall strip
Intensity at sample for Ei = 500 meV	5000 n cm^{-2} s^{-1} $\Delta\hbar\omega/E_i$ = 2% at elastic line 20000 n cm^{-2} s^{-1} $\Delta\hbar\omega/E_i$ = 5% at elastic line
Sample environment	Accepts all standard ISIS sample environment equipment
Data acquisition	Alphastation 500MHz personal workstation running VMS

i Beamline and Moderator

MAPS is situated on the S1 beamline viewing the ambient water moderator because the horizontal high angle bank of detectors on MAPS limited its construction to sites adjacent to the extracted proton beamline. A horizontal high angle bank means that this bank can be used with the full range of ISIS sample environment equipment.

ii Flight Paths

Optimisation of three critical distances naturally arise in the design of a chopper spectrometer: the moderator to chopper distance l_0, the chopper to sample distance l_1 and the sample to detector distance l_2. The considerations that affect the choice of l_0, l_1 and l_2 on the various contributions to the resolution function have been comprehensively dealt with by Perring [6]. The choice of these parameters for MAPS [see table 1] resulted from an optimisation based on minimising the

resolution widths whilst striving to maximise the flux or count rate. For l_1 and l_2 this is straightforward:

- The secondary flight path l_2 should be as large as possible. If the solid angle of a detectors is fixed at its desired value then both the fractional energy and Q resolutions improve with increasing l_2. Engineering and cost constraint then set the value of l_2; on MAPS this is 6m.

- The chopper to sample distance l_1 should be as short as possible to minimise the moderator contribution to the energy resolution. A lower bound is set on this distance because the chopper acts as a source of background. This means that there should be no direct line-of-sight from the innermost detectors to the Fermi chopper. On MAPS l_1 is 1.80m.

The optimisation of the chopper to moderator distance l_0 and open time of the chopper depends on the choice of other parameters (e.g. incident energy, secondary flight-path l_2 etc.) but there is, in general, a preferred value of l_0. For the optimisation of l_0 on MAPS the starting point was MARI. With all else equal, the increase of l_2 from 4m on MARI to 6m on MAPS results in an improved energy resolution. This improvement can be exploited by those experiments that need it, or it can be exchanged for enhanced flux, by increasing the opening time of the chopper, yet retaining the same resolution as MARI. For an energy resolution in the range 2-4% the optimised value of l_0 in the range 9m to 11m. The MAPS design has l_0 at 10m.

iii Instrument Furniture

MAPS has several features to assist single crystal experiments:

- The Fermi chopper is supported by a automatic jack system that moves it in and out of the beam in a few minutes, without breaking the instrument interlocks. The swift switching between a monochromatic and white beam on the sample aids the alignment and checking of the crystal orientation both at the start of and during an experiment.

- A automatic three-position attenuation device has been installed. The ability to ensure that an Bragg reflection is not saturating the detectors without having to manually install an attenuator has speeded up the alignment of the crystals.

- MAPS has two sets of beam defining jaws, to allow horizontal and vertical adjustment of the beam profile just before the Fermi chopper and sample. These jaws greatly improve the background by allowing removal of extraneous material from the direct beam (such as sample can material).

iv MAPS Vacuum Vessel

The MAPS vacuum vessel is a major piece of engineering. At $37m^3$ MAPS has the largest vacuum tank for a neutron instrument at ISIS (see figure 1). Two features of its design have important implications for single crystal neutron spectroscopy:

- The obstruction to the detectors view of the sample has been minimised through careful positioning of the main structure of the tank and the use of large areas of unsupported aluminium windows. This required considerable research into the mechanical properties of aluminium alloys for the window material.

- The MAPS vessel is a single volume. Unlike HET and MARI it does not have a thin internal aluminium window dividing the vessel into a sample tank and detector tank. On those spectrometers the window allows a high vacuum ($1x10^{-6}$ mbar) to be achieved in the sample tank which minimises the condensation of gases on the cryogenically cold samples. Scattering from such condensation, especially ice, can be a major source of structured background. Maintaining a cryogenic vacuum in such a large vessel is a challenge, but exclusion of the thin window from the direct neutron beam on MAPS removes a significant source of background in the inelastic spectra.

v Detector and Data Collection System

The MAPS detector system [11] is one of the biggest and most complex constructed on a neutron scattering instrument. It consists of 576 ^{3}He resistive wire position sensitive detectors that divide the 16 m^2 area into 147,456 individual pixel elements.

The detector system is highly stable, both temporally and spatially, has the same detection efficiency (at all neutron energies) as the standard ^{3}He detectors on existing ISIS chopper spectrometers, and the of the detectors along their length that is narrower than their width (see table 2). The detector system quickly recovers from saturation by highly intense elastic Bragg reflections from the single crystal sample so that they do not distort or impede the measurement of the inelastic response, which is many orders of magnitude lower

The accuracy, reliability and speed of the MAPS detector electronics is due to three aspects of the design

- The pre-amplifiers were chosen with an emphasis on low noise, low impedance and wide bandwidth characteristic to ensure that they introduced minimal distortion to the signal, leading to greater accuracy in the position encoding.

- The electronics that encode positional information employs an approach, where the incoming signals are firstly rapidly digitised and then processed by a programmable logic array using a look-up table held in an EPROM. This enables the MAPS system to be fast whilst still maintaining the required accuracy.

- The MAPS electronics uses high tolerance components throughout, and has placed an emphasis on simplicity of design. This has lead to a system with high reliability and reduced maintenance, which is essential with such a large number of detectors.

Table 2: Summary of PSD Parameters and Performance

Type	Resistive wire 10 atm (partial pressure) ^{3}He proportional counters
Physical size	25.4mm diameter by 0.4m, 1.0m and 1.3m
FWHM resonse along length	14 mm
Efficiency (w.r.t. standard 30cm 10 atm ^{3}He tube)	100%
Quiet Count (per 30cm length)	3 counts/hour (same a standard 30cm 10 atm ^{3}He tube)
Total circuit deadtime	1μS individual 5μS multiplexed
Positional Stability	< ± 0.2 channels in 4 months (≈ 3mm)
Resolution Stability (change in the FWHM measured at the same position)	≈ 0.15 channels in 4 months (≈ 2mm)

The MAPS detectors are divided into two banks [see figure 1]. A forward angle bank provides complete coverage over all azimuthal angles from 3° to 20° (this extends to 30° in the corners) and a high angle bank that extends the horizontal detectors from 20° to 60°. The concentration of detectors in the forward direction is because MAPS has been designed to examine magnetic materials, and the magnetic signal decreases with momentum transfer due to the magnetic form factor.

Such a vast number of pixels when combined with approximately 2000-2500 time-of-flight channels per pixel results in an extremely large data acquisition requirement. The size of the raw data file is 0.5Gb. Data acquisition is carried out in the next generation ISIS data acquisition electronics, DAE-II.

vi Data Visualisation and Analysis

The MAPS computer is a DEC Alpha-station 500MHz personal workstation, running VMS in the same instrument control program as other ISIS instruments. Initial data reduction in carried out on this machine using the current suite of programs common to HET and MARI. Visualisation and manipulation of the reduced data set, which is typically 120Mb in size, is carried out on a high specification PC (733Mhz, dual processor, 1Gb RAM) running a program written in the commercial Matlab software language. Software to fit models of the cross-section to the data, accounting for the instrument resolution is available for VMS, PC or Unix systems.

The key element in the philosophy of the MAPS design is the flexibility that a pixellated detector gives the experimenter. The time-of-flight and the pixel position of the scattered neutrons is stored in an array of ~10^8 pixels, from which the scattering function is constructed, in software, in a volume of reciprocal space divided into typically 10^7 volume elements. Through the graphical user interface of the visualisation software, MSLICE [12], the experimenter has complete freedom to construct scans along any direction in that reciprocal space volume and to project data onto any plane in reciprocal space. Whilst the resolution tuning is currently confined

to choosing the level of out-of-plane integration, we fully expect that in the future excitations will be optimally focussed (i.e. intensity of the signal of interest maximised with respect to other scattering processes), by creating bespoke resolution functions in software.

Model fitting to single crystal data taken on MAPS can be performed in the program TOBYFIT [13]. It combines and generalises the experience embodied in a number of model fitting programs written for HET and MARI over the past few years. It convolutes user-provided model scattering laws with the instrumental resolution function, and performs least-squares fits to experimental data. It can simultaneously fit a number of 1D cuts and 2D planes of data taken from each of several runs. As well as allowing the parameters in the model scattering law to be fitted, it can also be used to refine instrument parameters, for example the moderator pulse width, and any small misorientation of the sample.

III. MAPS First Measurements

The user programme started on MAPS in August 2000. This section presents some examples of data from the first experiments performed on the spectrometer. The aim is not to review the science or pre-empt the full analysis of the experimental data, but use it to show the power of the MAPS spectrometer and software.

i $KCuF_3$ [14]

$KCuF_3$ offers a physical realisation of a fundamental model magnetic system – a one-dimensional chain of spin–½ magnetic moments in which each ion is coupled antiferromagnetically to its neighbours by the Heisenberg interaction. The one-dimensional nature of $KCuF_3$ occurs because the S=½ Cu^{2+} ions are strongly coupled (exchange energy J = 17 meV) along the crystallographic c direction, but with much weaker interactions ($\approx 10^{-2} J$) in the a and b directions. The dynamics of the spins on the 1D chain of Cu atoms were studied a few years ago on MARI [9], and the data provided the first unambiguous evidence of the unconventional excitations in this extreme quantum system. Interest in idealised theoretical models has recently expanded to include the crossover from the quantum behaviour of isolated chains to the classical behaviour of 3D systems. Understanding the nature of the spin dynamics that accompany the crossover from 1D to 3D physics was the purpose of the investigation on MAPS.

In the experiment the sample was oriented with the *(0k0)* and *(00l)* directions in reciprocal space perpendicular to the incident beam. Figure 2 shows the excitation spectrum from $KCuF_3$ below 40meV taken in a slice perpendicular to *(0k0)* centred on k=0. It clearly shows the 1D dispersion along the chain direction (i.e. *(00l)*) as a function of energy. The pixellated detector on MAPS allows the excitations to be mapped right through zero momentum transfer along the chain direction, revealing in detail the branch emanating from this point for the first time.

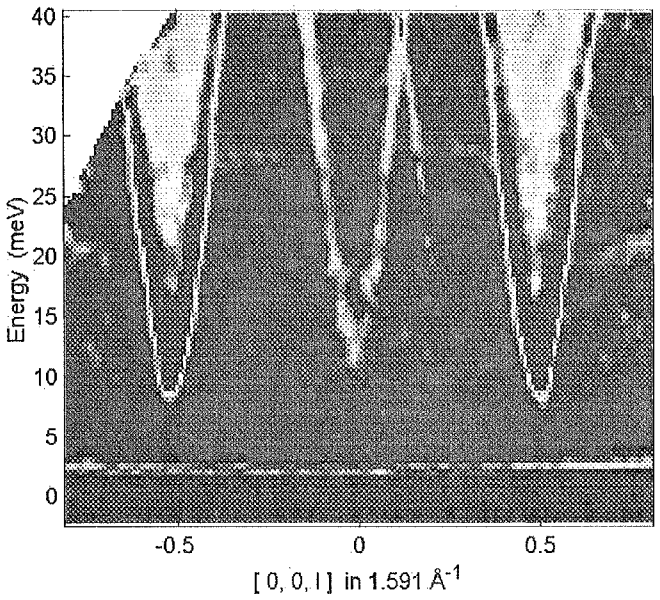

Figure 2: Excitation spectrum from $KCuF_3$ along the chain direction [14]

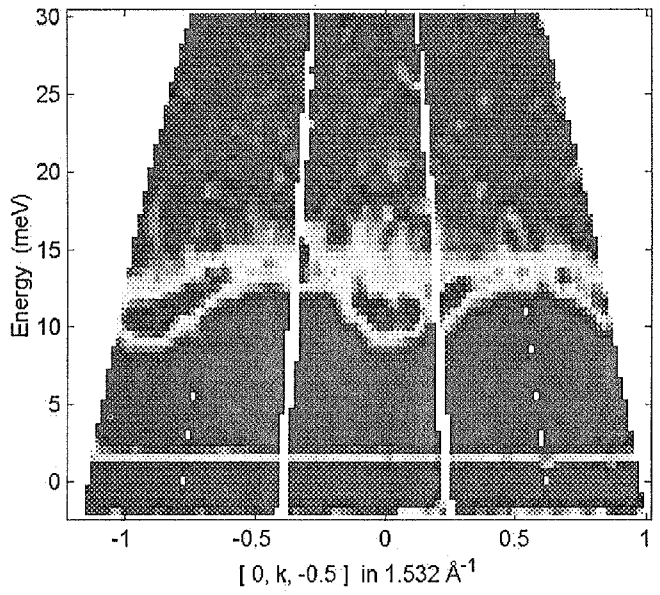

Figure 3: Excitation spectrum from $KCuF_3$ perpendicular to the chain direction [14]

Figure 3 demonstrates again the versatility of the pixellated detector on MAPS. Without having to make another measurement in a different configuration, a slice perpendicular to that taken in figure 2 can be made in software. Here a slice is shown that has been taken perpendicular to the chain direction at a value of l=-0.5. The effect of interchain interactions leading to a dispersion of the excitations perpendicular to the chains is clearly evident. On MARI and HET a measurement similar to that in figure 1 would integrate over a large part of this dispersion, due to the fixed size

of the detectors, thereby increasing the apparent energy width of the excitations in an uncontrolled fashion. On MAPS both the interchain dispersion can be measured *and* the level of integration in this direction can be controlled.

ii $CuGeO_3$ [15]

$CuGeO_3$ is another example of a one-dimensional system but which undergoes a phase transition at 14K that dimerises the one-dimensional chain of magnetic atoms, so that the interaction between successive ions in the chain alternate in size. MARI was used to investigate the high energy part of the excitation spectrum [16], showing the existence of a continuum of excitations above the sinusoidal dispersion relation expected for spin waves. MAPS, with its increased detector coverage and ability to allow the resolution to be tuned, showed that MARI did not in fact reveal the full story.

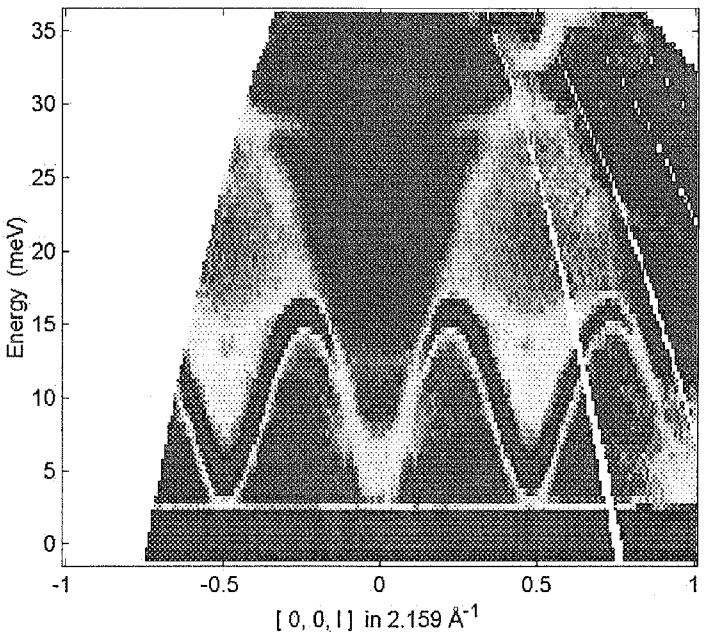

Figure 4: Excitation spectrum from $CuGeO_3$ along the dimerised chain direction [15]

Figure 4 shows the dispersion along the chain direction as a function of energy transfer in $CuGeO_3$. In addition to the spectrum observed on MARI [16], weak dispersive scattering can be seen between 25 and 35meV. The ability of MAPS to survey the excitation spectrum along the chain direction, and to permit an examination of the scattering in directions perpendicular to the chains without further measurement, enabled the scattering to be quickly identified as new dispersive features of the $CuGeO_3$ spectrum. The challenge now is to understand their physical origins.

iii $YBa_2Cu_3O_{7-d}$ [17]

The Cu-O planes in $YBa_2Cu_3O_{7-d}$ are stacked in weakly interacting bilayers so that the scattering intensity is modulated with zero intensity when l=0. On a prototype MAPS position sensitive detector system installed on HET it was demonstrated that the scattering intensity could be easily mapped as a function of (h,k,$l\neq$0) with the crystal set to one orientation [18]. This experiment revealed the orientation and symmetry of the incommensurate scattering and established its similarity to $La_{1-x}Sr_xCuO_4$.

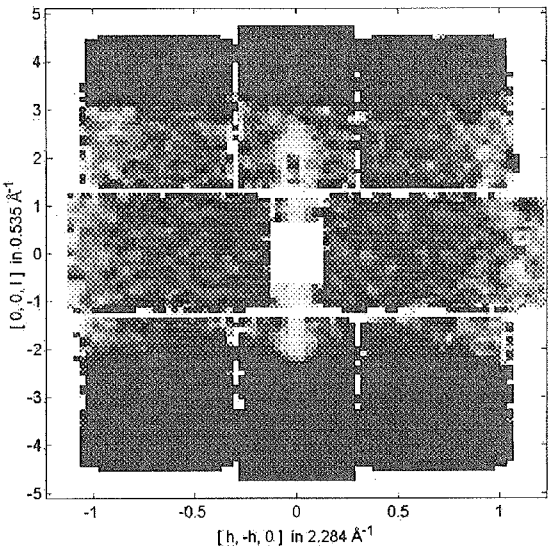

Figure 5: The 'resonance peak' in $YBa_2Cu_3O_{7-d}$ being studied as a function of magnetic field in a cryomagnet. The slice is over energy tranfer of 30-40meV [17]

The 'resonance peak', a resonant spin excitation occurring at an energy of 30-40meV which is conjectured to be intimately involved with the creation of the superconducting state has been the subject of intensive study over recent years, Figure 5 shows a study of the 'resonance peak' in $YBa_2Cu_3O_{7-d}$ as a function of magnetic field , where the increased detector coverage and pixellation on MAPS was able to give access to this peak and the improved resolution the possibility of determining whether the peak splits on application of a magnetic field.

iv Cobalt

Cobalt is an archetypical itinerant electron ferromagnet. In such systems, the long wavelength spin waves have a quadratic dispersion relation, but away from the zone centres the itinerant nature is expected to manifest itself as strong damping of the spin waves, and additional spin wave branches due to inter-band transitions. Figure 6 shows scattering data taken from hexagonal cobalt on MAPS, during commissioning of the detector electronics, when the detectors in the bottom right and very top right were not yet installed. The crystal was aligned

with the hexagonal planes perpendicular to the incident beam, which had energy 450 meV. Rings of scattering from spin waves are clearly seen around reciprocal lattice points of the form (h,k,3), with the 6-fold symmetry of the crystal evident in the data. The spin wave energies lie in the range 220-230 meV.

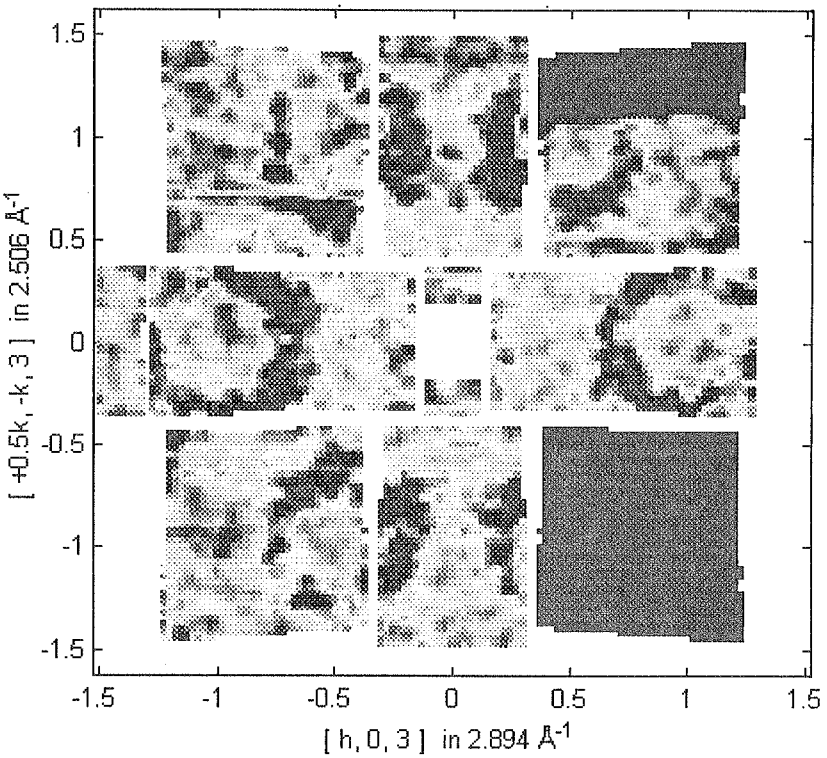

Figure 6: Spin waves in hexagonal Cobalt]

The dispersion relation has been modelled by that for a Heisenberg Hamiltonian:

$$H = -J \sum_{i,j} S_i . S_j \,, \qquad (1)$$

where S is the spin, [see figure 7]. To allow for a finite lifetime of the spin waves, the response has been broadened by that for a damped simple harmonic oscillator. The free parameters are the exchange constant, J, inverse lifetime, γ, and the intensity scale. The fitted values are $12JS = 199 \pm 7$ meV, and $\gamma = 69 \pm 12$ meV, which shows that the spin waves are heavily damped at excitation energies of 220 meV. From the same data set, slices can be taken in high symmetry planes yielding spin waves at other energies. For example, similar analysis shows $12JS = 185 \pm 5$ meV for excitations at 110 meV. It is evident that the dispersion relation is well modelled by that for the Heisenberg Hamiltonian. From just one setting of the crystal a broad survey of the spin waves from 50 to 250 meV can be performed, even in a 3D system.

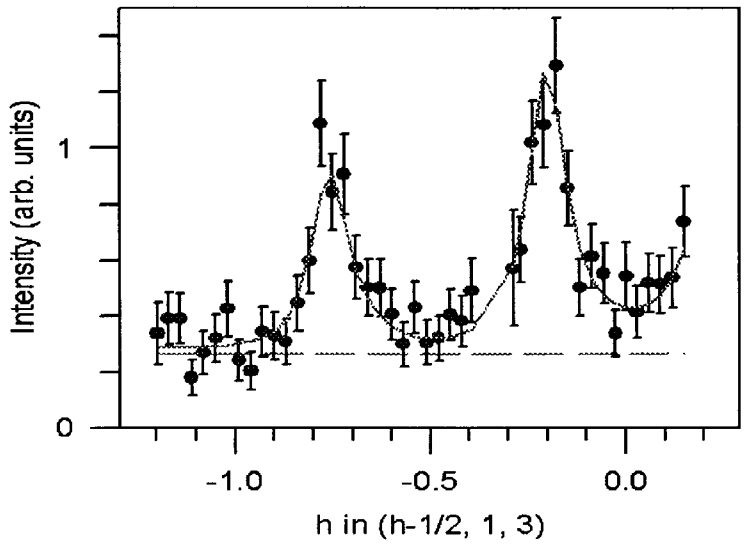

Figure 7: A cut parallel to (h,0,0) through the ring at the lower left part of figure 6. The solid line is the result of a fit performed in TOBYFIT.

IV. Conclusions

MAPS, the new state-of-the-art neutron scattering instrument at ISIS is already producing new results and approaches to inelastic neutron scattering.

Instruments like MAPS show that the performance of instruments is no longer necessarily defined by the quantity of neutrons, but also by the progress in the technology incorporated in their designs. Technological advances in electronics are driving neutron instrumentation forward, allowing the collection of increasingly large data sets.

This growth has mirrored the growth in computing capabilities which has allowed the manipulation and visualisation of the data produced in ever more imaginative and complex ways.

V. Acknowlegements

The construction of a new spectrometer such as MAPS relies on the efforts of a large number of people. We would like acknowledge the following people and members of the groups they lead at ISIS for their contributions to MAPS. Uschi Steigenberger, Julian Norris, Nigel Rhodes, Gary Thomas, Zoe Bowden and Kevin Knowles. We also thank the first users who have given us permission to present their unpublished data [14,15 ,18,19].

VI. References

[1] A.D. Taylor, B.C. Boland, Z.A. Bowden, Proc ICANS-IX (ed F Atchison and W Fischer) p349 (1987)

[2] A.D. Taylor, M.Arai, S.M. Bennington, Z.A. Bowden, R. Osborn, K. Anderson, W.G. Stirling, T.Nakane, K. Yamada, D. Welz, Proc ICANS-XI (ed M.Misawa, M.Furusaka, H.Ikeda and N.Watanabe) p705 (1990)

[3] S.M.Hayden, R. Doubble, G.Aeppli, T.G.Perring, E.Fawcett, Phys. Rev. Lett. **84,** p999-1002 (2000)

[4] P.C. Dai, H.A. Mook, S.M. Hayden, G. Aeppli, T.G. Perring, R.D. Hunt, F. Dogan, Science **284,** p1344-1347 (1999)

[5] M.Arai M, T.Nishijima, Y.Endoh , T.Egami, S.Tajima, K.Tomimoto, Y.Shiohara, M.Takahashi, A.Garrett, S.M.Bennington, Phys. Rev. Lett. **83**, p608-611 (1999)

[6] S.Itoh, Y.Endoh, K.Kakuria, H.Tanaka, Phys. Rev. Lett. **74**, p2375-2378 (1995)

[7] S.M.Hayden, G.Aeppli, H.A. Mook, T.G. Perring, T.E. Mason, S-W. Cheong, Z.Fisk, Phys. Rev. Lett. **76,** p1344-7, (1996)

[8] T.G. Perring, G.Aeppli, S.M. Hayden, S.A. Carter, J.P. Remeika, S-W. Cheong, Phys. Rev. Lett. **77**, p711-14, (1996)

[9] D.A. Tennant, T.G. Perring, R.A. Cowley, S.E. Nagler, Phys. Rev. Lett. **70**, p4003-6, (1993)

[10] T.G. Perring, *Contributions to the ESS Instrument Working Group on Single Crystal Spectroscopy – ESS-98-74-T,* (1998); T.G. Perring, Ph.D. Thesis, University of Cambridge (1991)

[11] C.D. Frost, R.S. Eccleston, J.Norris, N.J. Rhodes and D.J. White, Proc ICANS XIV (ed J.M. Carpe n ter and C.A. Tobin) p184 (1998)

[12] R. Coldea, the program 'MSLICE' (Fortran and Matlab)

[13] T.G. Perring, the program 'TOBYFIT' (Fortran)

[14] D.A. Tennant, B.Lake, R.Coldea, C.D. Frost, private communication.

[15] M.Arai, C.D.Frost, private communication

[16] M. Arai, M. Fujita, M. Motokawa, J. Akimitsu, S.M. Bennington Phys. Rev. Lett. **77** p3649 (1996)

[17] A.T.Boothroyd, P.Dai, H.A.Mook, private communication.

[18] H.A.Mook, P.Dai, S.M.Hayden, G.Aeppli, T.G.Perring, F.Dogan Nature **395**, p580-582 (1998)